Eur J Nucl Med Mol Imaging
DOI 10.1007/s00259-014-2939-8

ORIGINAL ARTICLE

^{18}F-GE-180: a novel TSPO radiotracer compared to ^{11}C-R-PK11195 in a preclinical model of stroke

Hervé Boutin · Katie Murray · Jesus Pradillo · Renaud Maroy · Alison Smigova · Alexander Gerhard · Paul A. Jones · William Trigg

Received: 17 June 2014 / Accepted: 8 October 2014

Abstract
Purpose Neuroinflammation plays a critical role in various neuropathological conditions, and hence there is renewed interest in the translocator protein (TSPO) as a biomarker of microglial activation and macrophage infiltration in the brain. This is reflected in the large amount of research conducted seeking to replace the prototypical PET radiotracer ^{11}C-R-PK11195 with a TSPO ligand with higher performance. Here we report the in vivo preclinical investigation of the novel TSPO tracer ^{18}F-GE-180 in a rat model of stroke.
Methods Focal cerebral ischaemia was induced in Wistar rats by 60-min occlusion of the middle cerebral artery (MCAO). Brain damage was assessed 24 h after MCAO by T2 MRI. Rats were scanned with ^{11}C-R-PK11195 and ^{18}F-GE-180 5 or 6 days after MCAO. Specificity of binding was confirmed by injection of unlabelled R-PK11195 or GE-180 20 min after injection of ^{18}F-GE-180. In vivo data were confirmed by ex vivo immunohistochemistry for microglial (CD11b) and astrocytic biomarkers (GFAP).
Results ^{18}F-GE-180 uptake was 24 % higher in the core of the ischaemic lesion and 18 % lower in the contralateral healthy tissue than that of ^{11}C-R-PK11195 uptake (1.5±0.2-fold higher signal to noise ratio). We confirmed this finding using the simplified reference tissue model (BP_{ND}=3.5±0.4 and 2.4 ±0.5 for ^{18}F-GE-180 and ^{11}C-R-PK11195, respectively, with R_1 = 1). Injection of unlabelled R-PK11195 or GE-180 20 min after injection of ^{18}F-GE-180 significantly displaced ^{18}F-GE-180 (69±5 % and 63±4 %, respectively). Specificity of the binding was also confirmed by in vitro autoradiography, and the location and presence of activated microglia and infiltrated macrophages were confirmed by immunohistochemistry.
Conclusion The in vivo binding characteristics of ^{18}F-GE-180 demonstrate a better signal to noise ratio than ^{11}C-R-PK11195 due to both a better signal in the lesion and lower nonspecific binding in healthy tissue. These results provide evidence that ^{18}F-GE-180 is a strong candidate to replace ^{11}C-R-PK11195.

Keywords Positron emission tomography · Translocator protein · R-PK11195 · Brain ischaemia · GE-180

Electronic supplementary material The online version of this article (doi:10.1007/s00259-014-2939-8) contains supplementary material, which is available to authorized users.

H. Boutin · A. Gerhard
Faculty of Medical and Human Sciences, University of Manchester, Manchester, UK

H. Boutin (✉) · A. Smigova · A. Gerhard
Wolfson Molecular Imaging Centre, University of Manchester, 27 Palatine Road, Manchester M20 3LJ, UK
e-mail: herve.boutin@manchester.ac.uk

K. Murray · J. Pradillo
Faculty of Life Sciences, University of Manchester, Manchester, UK

R. Maroy
SHFJ - CEA Orsay, Orsay, France

P. A. Jones · W. Trigg
GE Healthcare Ltd., Amersham, UK

Present Address:
J. Pradillo
Universidad Complutense/Politecnica de Madrid, Madrid, Spain

Introduction

Over recent decades, increasing evidence has supported the role of neuroinflammation as an essential contributor in CNS diseases, whether it is acute brain injury such as stroke [1, 2], chronic neurodegenerative diseases such as Alzheimer's disease [3–7], Parkinson's disease [8–11] or primary inflammatory disorders such as multiple sclerosis [12–14]. This has led to increasing interest in visualizing neuroinflammation in a noninvasive manner that would lead to a better understanding

Published online: 29 October 2014

of neuroinflammation, its time course and its role in brain diseases. So far, the most established and best characterized biomarker for in vivo imaging of neuroinflammation is the 18-kDa translocator protein TSPO, formerly known as peripheral benzodiazepine receptor [15]. Strictly speaking, TSPO overexpression reflects microglial cell activation and proliferation [16] rather than neuroinflammation in its broader sense. The characteristics of TSPO as a surrogate marker of neuroinflammation led to the development of ^{11}C-R-PK11195 as a TSPO PET ligand in the early 1980s [15, 17]. ^{11}C-R-PK11195 has the disadvantages of the short half-life of ^{11}C, a relatively poor signal to noise ratio due to high nonspecific binding (for review see Chauveau et al. [15]) and a rather problematic radiochemistry, although this last point is poorly documented despite being well known by the radiochemistry community. To compensate for the poor binding properties of ^{11}C-R-PK11195, advanced modelling techniques have been implemented to extract as much information as possible from the PET images when no anatomical reference tissue can be defined [18–20]. For these reasons and its long-lasting presence in the field of clinical TSPO PET imaging, ^{11}C-R-PK11195 is still the most used TSPO radiotracer in clinical studies [15].

Over the last decade, the issues with ^{11}C-R-PK11195 and the increased interest in neuroinflammation have triggered a renewed effort to develop improved TSPO PET tracers, and numerous compounds have been developed during this period [15, 21, 22]. Most of these tracers, such as ^{18}F-FEDAA1106, ^{11}C-PBR28, ^{11}C-DPA-713 and ^{18}F-DPA-714, have a better signal to noise ratio than ^{11}C-R-PK11195 in PET imaging of various animal models [15, 23]. However, some studies with these tracers clearly indicate variable results among different models and the need to perform direct comparisons of two tracers (i.e. scanning the same animal or subject twice) [15, 23, 24]. More recently, these new tracers have been investigated in various clinical studies, some of which have yielded different results depending on the tracer used [14, 25] or the disease studied [25, 26].

Taken altogether, the preclinical and first clinical studies mentioned above highlight the need for thorough evaluation of these new tracers with the expectation that some of them will be introduced at clinical level on a wider scale. Initial preclinical evaluation should provide information about the potential of a new TSPO PET tracer, but do not guarantee success in the clinic. Ideally, clinical evaluation of the tracer should follow, comparing it with ^{11}C-R-PK11195 in a disease for which microglial activation is sufficiently described to prevent any bias.

We report here the in vivo evaluation of a new tetrahydrocarbazole TSPO tracer, ^{18}F-GE-180 (*S*-*N*,*N*-diethyl-9-2-^{18}F-fluoroethyl]-5-methoxy 2,3,4,9-tetrahydro-1H-carbazole-4-carboxamide [27]), and its direct comparison (i.e. in the same animals) with ^{11}C-R-PK11195 in a rat model of stroke. To put our study into context, we also compared our data with those recently reported by Dickens et al. [28], who compared the two tracers in a different strain of rats and in a different (lipopolysaccharide-induced) model of neuroinflammation. We also provide novel information about the metabolism of ^{18}F-GE-180.

Materials and methods

Induction of focal cerebral ischaemia in rats

Studies were conducted in ten male Wistar rats (Charles River, Margate, UK). The animals weighed 357±44 g. The animals were kept under a 12-h light/dark cycle with free access to food and water. All procedures were carried out in accordance with the Animals (Scientific Procedures) Act 1986, and the specific project licence was approved by the UK Home Office. Focal cerebral ischaemia was induced by 60-min transient occlusion of the right middle cerebral artery (MCAO) by the insertion of a monofilament (Doccol Corporation, Sharon, MA) as previously described [23] (for full details see Supplementary material).

MRI

The primary outcome was infarct volume measured on MRI 24 h after transient MCAO. Animals were scanned using a Magnex 7-T, horizontal-bore magnet (Agilent Technologies, Oxford Industrial Park, Yarnton, UK) connected to a Bruker Biospec Avance III console (Bruker Biospin Ltd., Coventry, UK) with a transmit/receive 2.5 cm surface coil. Rectal temperature and respiration rate were monitored. Reperfusion of the right MCA was assessed using a FLASH-TOF-2D sequence. A T2-weighted fast spin echo sequence based on RARE was used to measure brain damage [29, 30] (details of the sequences can be found in the Supplementary material). Lesion volume was determined with Anatomist software (http://brainvisa.info/), Regions of interest (ROIs) corresponding to the infarcted tissue were delineated on the T2 MRI scans based on the enhanced contrast of oedematous tissue when compared with healthy tissue 24 h after MCAO.

PET and data acquisition

Rats were anaesthetized 5 to 6 days after MCAO by isoflurane inhalation (induction 5 % and thereafter 2 – 2.5 %) in oxygen. As a control, five naive rats (no MCAO) were scanned with ^{18}F-GE-180. All compounds were injected intravenously into a tail vein as a bolus. All injected doses, amounts of tracer injected and specific activities are provided in Supplementary Table 1.

Dual ^{11}C-R-PK11195/^{18}F-GE-180 scans

Six animals were scanned sequentially with ^{11}C-R-PK11195 and ^{18}F-GE-180 within 24 h (four rats were scanned with ^{11}C-

R-PK11195 first and then with ^{18}F-GE-180 3 h to 6 h later, and two rats were scanned with ^{18}F-GE-180 first and then with ^{11}C-R-PK11195 the following day). ^{11}C-R-PK11195 and ^{18}F-GE-180 were synthesized as described elsewhere [27, 31, 32].

Displacement study

To assess the specificity of ^{18}F-GE-180 in vivo, a displacement study was performed by injecting an excess (1 mg/kg) of either unlabelled R-PK11195 or GE-180 during the PET acquisition 20 min after the injection of ^{18}F-GE-180. Three rats were scanned twice with ^{18}F-GE-180 within 24 h, once with administration of unlabelled R-PK11195 and once following administration of GE-180 as unlabelled ligand 20 min after injection of ^{18}F-GE-180.

Data acquisition

The scans were performed on a Siemens Inveon® PET/CT scanner. A CT scan was performed prior to the PET acquisition to obtain the attenuation correction factors. The list mode acquisition data files were histogrammed into 3D sinograms and reconstructed using OSEM3D (details of the PET protocols can be found in the Supplementary material). Respiration and temperature were monitored throughout using a pressure-sensitive pad and rectal probe (BioVet; m2m Imaging, Cleveland, OH). Body temperature was maintained (37±0.7 °C) by the use of a heating and fan module controlled by the rectal probe via the interface controlled by the BioVet system.

At the end of the last PET scan, rats were quickly decapitated and the brains were quickly removed and immediately frozen in isopentane in dry ice. The brains were stored at −80 °C until cut with a cryomicrotome into adjacent 20-μm thick coronal sections. Brain sections were then stored at −80 °C until used for autoradiography or immunohistochemistry.

Image analysis

PET images were analysed using two sets of ROIs. The first set of ROIs came from automatic segmentation of the PET images using the local means analysis method [33] with partial volume effect correction using the geometric transfer matrix method and the ROIopt methods [23, 33–35]. Automatic segmentation of the volume had the advantage of delineating user-independent ROIs. For both tracers the following five ROIs were automatically segmented and labelled as: (1) core (ROI covering the core of the infarct in the MCAO territory and/or with the highest uptake), (2) edge-1 (ROI around the core ROI and/or with the second highest uptake), (3) edge-2 (ROI around the core ROI and/or with the 3rd highest uptake), (4) edge-3 (ROI around the core ROI and/or with the 4th highest uptake), (5) contralateral ROI (ROI with the lowest uptake), and (6) skull edges (ROI located on the edge of the skull; this ROI was not included in the data analysis). In control animals, two ROIs within the whole brain were segmented, a higher uptake ROI near the cerebroventricular zones and a lower uptake ROI corresponding to the rest of the brain (data not shown). The second set of ROIs was obtained from the anatomical ROIs used for quantification of the infarct volume on the T2 images (as described in the MRI section).

To coregister the T2 MRI and PET/CT images, a brain mask was delineated on each individual T2 MRI and CT image, and the resulting brain masks were then coregistered using rigid registration with mutual information. All methods were applied using the BrainVisa/Anatomist framework (http://brainvisa.info/). The cerebellum and olfactory bulbs were delineated based on the coregistered MRI images. ^{11}C-R-PK11195 and ^{18}F-GE-180 uptake was quantified using both the segmented and MRI-based ROIs.

Plasma and brain metabolite analysis

Male Wistar rats (200 to 250 g body weight) were anaesthetized using isoflurane in oxygen. ^{18}F-GE-180 (20 MBq) was administered intravenously by bolus injection into a tail vein of each rat. The rats were allowed to recover from the anaesthesia. Immediately before they were killed, the rats were further anaesthetized and then killed by cervical dislocation at 10, 30 or 60 min after injection (three rats per time-point). Blood and brain were immediately collected for processing and HPLC analysis (full details of the methods are provided in the Supplementary material).

Immunohistochemistry

In all the rats used in the PET study, astrogliosis and microglial activation were checked by immunohistochemistry staining for GFAP and CD11b, respectively (details of the method are provided in the Supplementary material).

Autoradiography

^{18}F-GE-180 (240.3 GBq/μmol, 1 nM) autoradiography was performed using 20-μm brain sections. Using adjacent sections, specific binding for TSPO was assessed by adding an excess of unlabelled R-PK11195 or unlabelled GE-180 (20 μM). Sections were preincubated in Tris buffer (Trizma Pre-set crystals, adjusted to pH 7.4 at 4 °C or room temperature, 50 mM, with 120 mM NaCl; Sigma-Aldrich, Gillingham, UK) at 4 °C for 5 min, then incubated for 60 min in Tris buffer at room temperature and then rinsed twice for 5 min with unlabelled buffer, followed by a quick wash in unlabelled distilled water and drying before exposure to a Phosphor-

Imager screen for 2 h. Autoradiographs were visualized using AIDA software (Raytest, Straubenhardt, Germany).

Statistical analysis

The paired Wilcoxon test was used to compare ^{11}C-R-PK11195 and ^{18}F-GE-180 uptake values for each ROI and to compare ROIs for each tracer using images summed from 40 to 60 min after injection. The unpaired Mann-Whitney test was used to compare the ^{18}F-GE-180 uptake values with and without injection of unlabelled tracer on images summed from 40 to 60 min after injection. All statistical calculations were performed with Statview 5.0.1 software (SAS Institute Inc., Cary, NC). All data are expressed as means±SD.

Results

Infarct volumes

As assessed by MRI, all animals except one had infarcts involving the whole striatum, and to some extent part of the cortical areas, most often the piriform cortex (Fig. 1). One animal was excluded from the study because of a very small infarct observed on the T2 images. The average infarct volumes without this animal were 65.7±12.7 mm^3 and 66.8±63.0 mm^3 for striatal and cortical infarcts, respectively, and 132.5±61.9 mm^3 for the total infarct.

PET imaging

As shown Fig. 2, the uptake of ^{18}F-GE-180 was significantly higher (+24 %) in the core of the infarct and significantly lower (−18 %) in the contralateral ROI than the uptake of ^{11}C-R-PK11195, leading to a significant increase of 1.5±0.2-fold in the core to contralateral ratio (Fig. 2d). ^{18}F-GE-180 brain uptake in normal animals (0.082±0.026 %) was not significantly different from that in the contralateral ROI of stroke animals (0.104±0.016 %). Using ROIs drawn on the T2 MRI images to quantify the PET images yielded the same results (see Supplementary Fig. 1), although automatic PET segmentation allowed the detection of an intermediate level of TSPO expression on the edges of the infarct core (Supplementary Fig. 2), ROIs that could not be identified on anatomical MRI.

The simplified reference tissue model showed that the binding potential (BP_{ND}) of ^{18}F-GE-180 was significantly

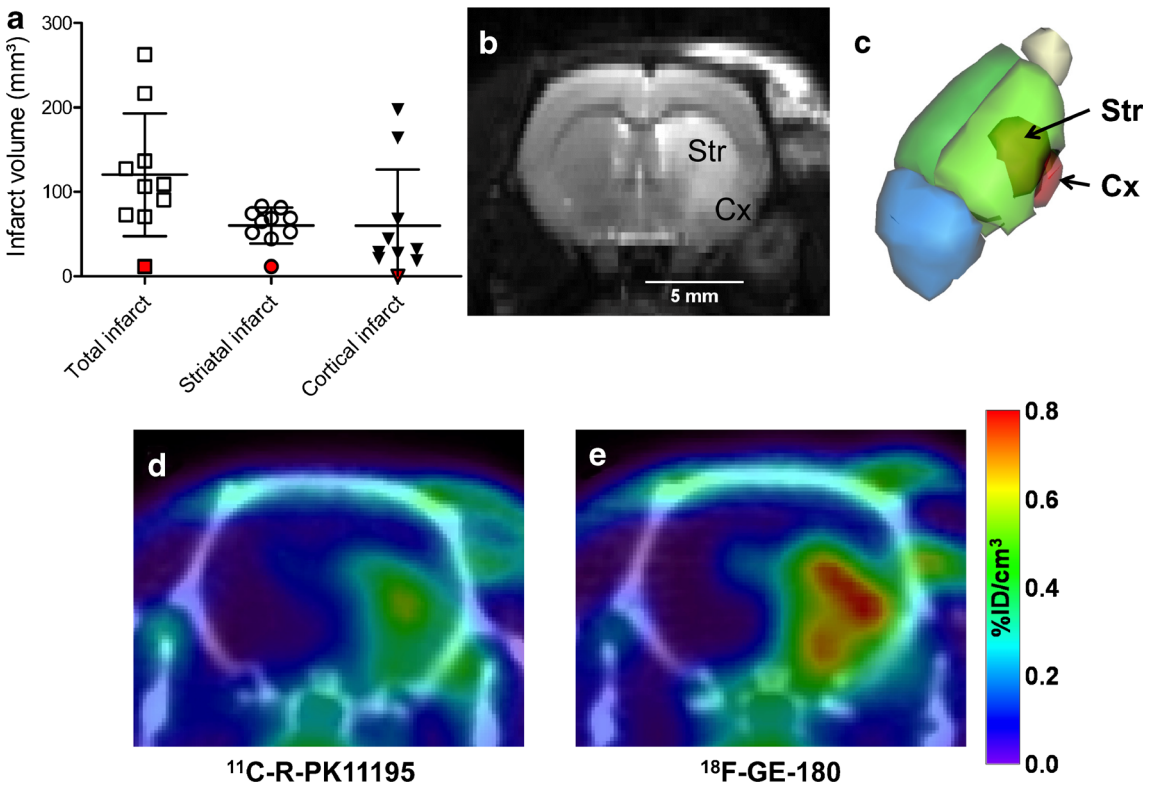

Fig. 1 Infarct areas on MRI. **a** Infarct volumes (together with the means ±SD, n=10) as measured by T2 MRI imaging 24 h after MCAO (the *red points* represent the only animal excluded from the PET study because of a very small infarct. **b** Representative T2 MR image in a rat with the infarct visible as an oedematous area with enhanced contrast (*white*; *Str* striatum, *Cx* cortex). **c** 3D rendering of the infarct areas measured in the animal shown in **b** with the cortical (*Cx*) and striatal (*Str*) infarct shown in red and by transparency through the ipsilateral healthy tissue (*light green*); *dark green* contralateral side, cerebellum and olfactory bulbs are respectively shown in *light yellow* and *blue*. **d**, **e** Coregistered quantitative PET/CT images (**d** ^{11}C-PK11195, **e** ^{18}F-GE180) of the same animal (PET images summed from 40 to 60 min after injection)

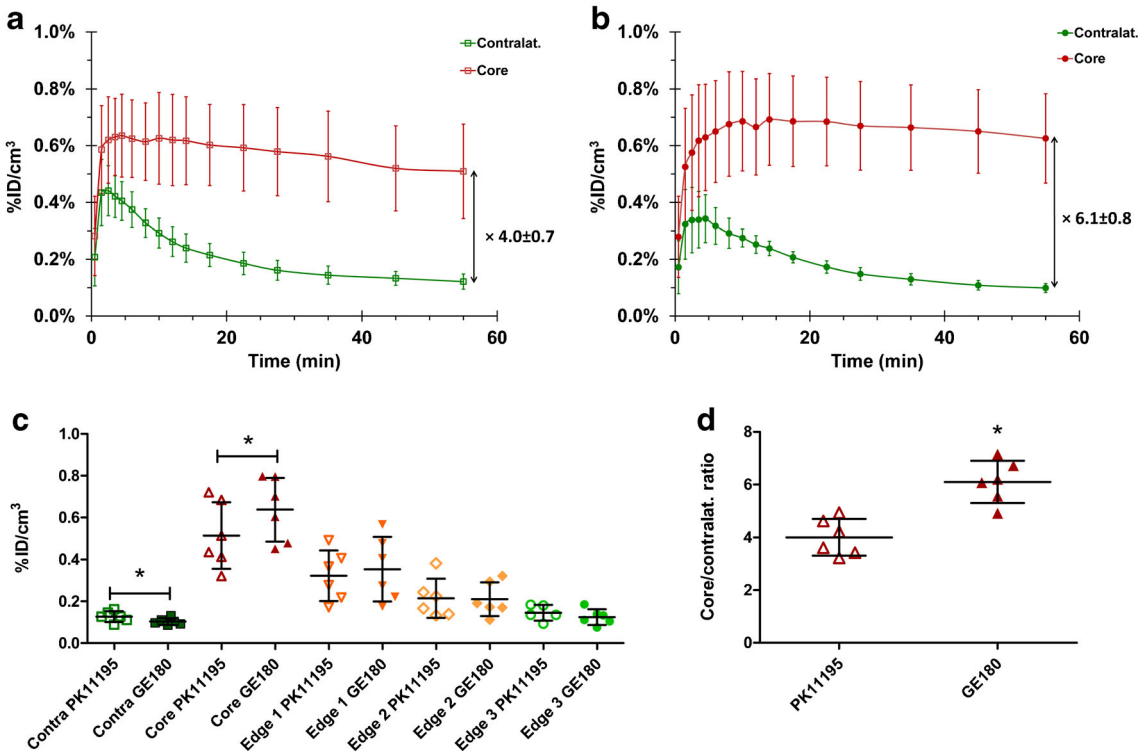

Fig. 2 ^{11}C-R-PK11195 and ^{18}F-GE-180 uptake. **a**, **b** Uptake (mean±SD) over the 60 min after injection in the infarct core and the contralateral side (**a** ^{11}C-R-PK11195, **b** ^{18}F-GE-180). The difference between the lesion core and contralateral ROI was greater for ^{18}F-GE-180 than for ^{11}C-R-PK11195 (6.1-fold vs. 4.0-fold, respectively). **c** Quantification of uptake on images summed from 40 to 60 min after injection shows significantly lower uptake in healthy tissue (*dark green*) and a significantly higher uptake in the lesion for ^{18}F-GE-180 (*dark red*). **d** Infarct core to contralateral uptake ratios. *$p<0.05$ between groups ($n=6$), paired Wilcoxon test

higher than that of ^{11}C-R-PK11195 in the infarct core (5.3±1.2 vs. 2.8±0.7). However, R_1 (tracer delivery ratio between the chosen ROI and the reference ROI) values were >1 for both tracers in the lesion core, suggesting faster delivery than in the reference (healthy) tissue. To account for this, we measured the BP_{ND} with the R_1 value fixed at 1. This significantly reduced the BP_{ND} for both tracers but the difference between the BP_{ND} for ^{18}F-GE-180 and that for ^{11}C-R-PK11195 remained significant (3.5±0.4 vs. 2.4±0.5).

Injection of an excess of unlabelled ligand significantly displaced ^{18}F-GE-180 in the infarct (69 %±5 % and 63 %±4 % of the uptake before injection of the unlabelled ligand for R-PK11195 or GE-180, respectively; Fig. 3 and Table 1). Injection of unlabelled ligands significantly reduced the mean uptake values from 40 to 60 min in the striatal infarct and these values were not significantly different from those in the contralateral ROIs (Table 1). Uptake values in the contralateral side after injection of unlabelled R-PK11195 or GE-180 were not affected by injection of unlabelled tracer (Table 1), confirming that the contralateral tissue was devoid of specific binding, and could therefore be used as the reference tissue for modelling.

Plasma and brain metabolite analysis

Following intravenous administration of ^{18}F-GE-180, the percentage of radioactivity in the plasma that was due to the

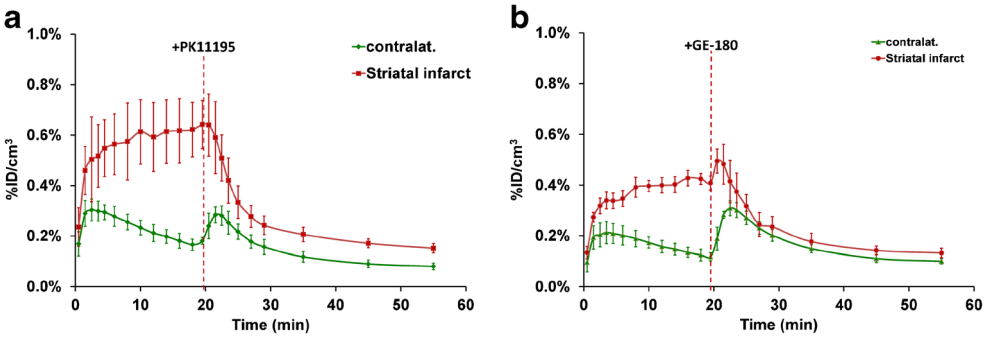

Fig. 3 Time–activity curves of ^{18}F-GE-180 in the ipsilateral (infarcted) striatum and contralateral side before (0–20 min) and after (>20 min) intravenous injection of an excess of unlabelled (1 mg/kg) PK11195 (**a**) or GE-180 (**b**) (three animals, same animals scanned at 5 and 6 days after MCAO). ROIs were drawn on the T2 MR images 24 h after MCAO

Table 1 Mean (±SD) uptake values from 40 to 60 min after injection of ^{18}F-GE-180 with and without injection after a further 20 min of unlabelled PK11195 or GE-180 (expressed as %ID/cm^3) using ROIs delineated on T2 MRI images

	^{18}F-GE-180 (n=6)	^{18}F-GE-180+PK11195 (n=3)[a]	^{18}F-GE-180+GE-180 (n=3)[a]
Contralateral ROI	0.108±0.018 %	0.098±0.014 %	0.111±0.012 %
Striatal infarct	0.603±0.175 %*	0.131±0.012 %**	0.124±0.013 %**

*p<0.05 vs. contralateral ROI (paired Wilcoxon test); **p<0.05 vs. ^{18}F-GE-180 alone (unpaired Mann-Witney test)

presence of parent compound decreased with time, such that 21 % remained by 60 min after injection (Table 2). Radiolabelled metabolite M1, accounted for 21 % of the total activity in the plasma 10 min after injection, with the proportion increasing with time to 53 % by 60 min after injection. Two other more minor metabolites were observed 10 and 30 min after injection of ^{18}F-GE-180 increasing to 5 % and 21 % of total plasma activity by 60 min after injection. In contrast, the metabolites observed in the plasma are not formed in the CNS nor do they cross the blood–brain barrier (BBB) to any significant degree. In the brain not less than 95 % of the radioactivity was attributable to the parent compound, even 60 min after injection (Table 2).

Immunohistochemistry and autoradiography

Immunohistochemistry revealed the presence of CD11b-positive cells (activated microglial cells and infiltrated macrophages) in the core of the lesions and GFAP-positive cells (astrogliosis) on the edge of the core ischaemic lesions (Fig. 4). TSPO binding was confirmed in vitro by autoradiography using ^{18}F-GE-180 (1 nM) and the specificity of binding was confirmed by displacement with excess of unlabelled R-PK11195 or GE-180 (1 μM) (Supplementary Fig. 3).

Discussion

As we have recently demonstrated in animal models [23], and even more so in human conditions in which high interindividual variability in size and/or location of the infarct is expected [36, 37], direct comparison of PET tracers in the same subject by performing successive scans within 24 h is the most robust way of comparing the performance of two tracers such as ^{18}F-GE-180 and ^{11}C-R-PK11195.

In our study, ^{18}F-GE-180 had a significantly higher uptake in the infarct and importantly a lower uptake in healthy tissue, leading to a significantly better infarct/contralateral ratio, than ^{11}C-R-PK11195. Interestingly, the facts that uptake values in the contralateral ROI (0.108±0.018 %) were not significantly different from those in control animals (0.082±0.026 %) and that injection of an excess of unlabelled R-PK11195 or GE-180 yielded identical values to those obtained without displacement (Table 1) demonstrates that the contralateral ROI did not contain specific binding and could therefore be used as a reference tissue. In the ischaemic striatum, the average uptake values (40 – 60 min summed image) were not significantly different from the values in the contralateral ROI (Table 1) following injection of an excess of unlabelled R-PK11195 or GE-180, but the time–activity curve showed that the uptake values were not identical to those observed in the contralateral ROI either. This suggests that there was a higher level of nonspecific binding in the infarct and/or that a small fraction of the metabolites may have entered the brain through the disrupted BBB.

Our metabolite study showed that ^{18}F-GE-180 has blood pharmacokinetics similar to those of other new TSPO tracers such as ^{11}C-DPA-713 or ^{18}F-DPA-714, with 70 %, 40 % and 21 % of the parent compound still present at 10 min, 30 min and 60 min after injection, respectively [38, 39]. Similar to many of the new TSPO tracers, metabolites were barely

Table 2 Relative percentages of metabolites and parent compound ^{18}F-GE-180 found in plasma and brain extracts at 10, 30 and 60 min after injection (three animals per time-point)

	HPLC retention time (min)	Plasma			Brain		
		Time after injection (min)			Time after injection (min)		
		10	30	60	10	30	60
Metabolite M1	3.1	21±25	41±19	53±14	1±2	4±3	5±3
Metabolite M2	6.3	9±9	15±0	21±6	1±1	1±0	1±1
Metabolite M3	7.3	Not detectable	4±6	5±4	1±0	Not detectable	<1
^{18}F-GE-180	11	70±18	41±16	21±4	98±2	96±3	94±2

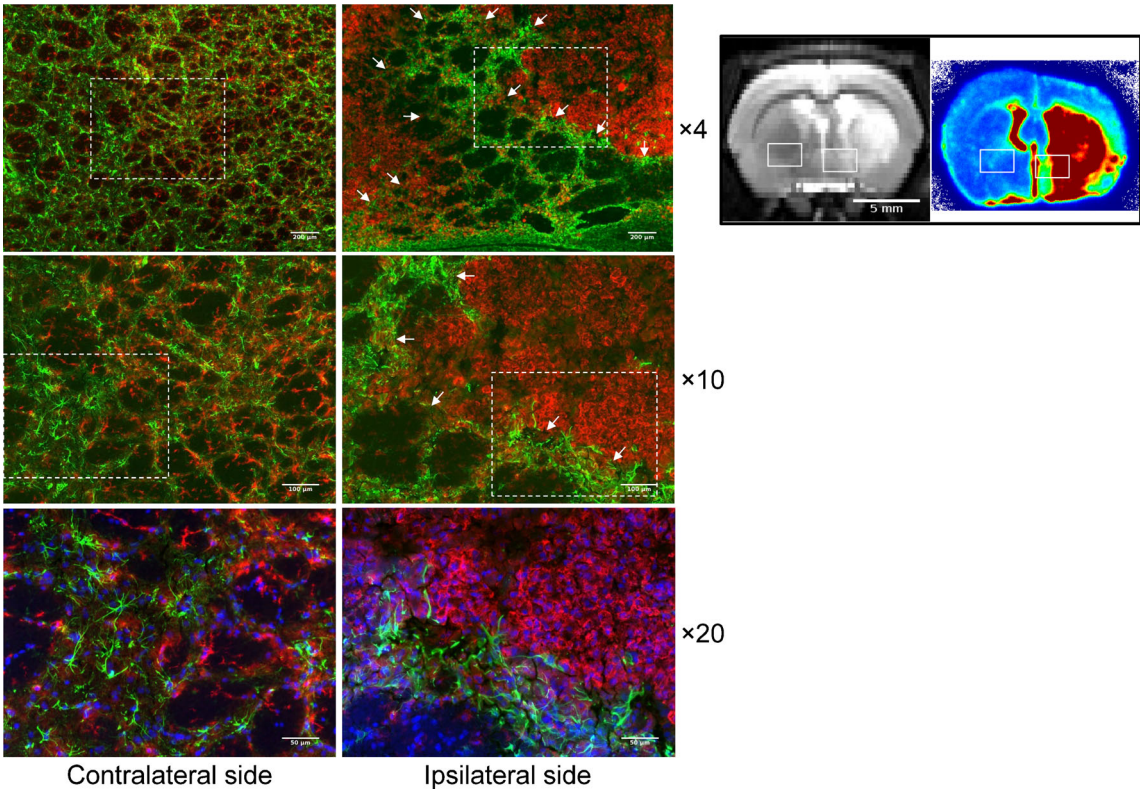

Fig. 4 Representative immunohistochemical staining of microglial and infiltrated macrophages with CD11b (*red*), astrocytes with GFAP (*green*) and nuclear staining with DAPI in the contralateral (*left*) and ipsilateral (*right*) sides of the brain of a rat 6 days after MCAO. *Scale bars*: from top to bottom, 200 μm, 100 μm and 50 μm. The *inserts* (*top right*) shows the approximate location of the fields of view used for immunohistochemistry (*white rectangles*) on the MRI and [^{18}F]GE-180 autoradiographic images from the same animal

detectable in healthy brain, supporting the view that quantification of TSPO using ^{18}F-GE-180 reflects the level of TSPO expression unbiased by nonspecific uptake of metabolites. We cannot, however, exclude the possibility that some metabolites crossed the *disrupted* BBB after stroke. This is supported by modelling the data using the SRTM which showed $R_1 > 1$, indicating faster tracer delivery in the infarct probably due to BBB disruption after stroke that we have previously demonstrated [23].

Regarding the potential effect of repeated administration of a nontracer dose (1 mg/kg) of TSPO ligands, we did not observe a systematic change in the animals in TSPO binding 6 days after MCAO (second scans) following administration of cold ligand at 5 days after MCAO, which suggests that this dose of cold ligand did not affect the expression of TSPO. Assessing the potential effect of repeated administration of unlabelled ligand at doses used for displacement studies (1 – 5 mg/kg), similar to those used in therapy for example, was outside the scope of the present work and would require further characterization.

Our modelling data confirmed the raw uptake data and showed 1.5±0.2-fold higher BP values for ^{18}F-GE-180 than for ^{11}C-R-PK11195. The location and specificity of the binding was also confirmed by in vitro autoradiography, and coincided with an increased number of activated microglial cells and infiltrated macrophages in the infarct, and an astrocytic scar around it as shown by the immunohistochemistry.

Overall, the results presented here are in good agreement with those recently reported by Dickens et al. [28] who used a different model of neuroinflammation, and support further use of ^{18}F-GE-180 in preclinical and clinical imaging of TSPO. Although ^{11}C-R-PK11195 is still widely used clinically and preclinically [15, 21, 40], the present results are in line with previous observations made by our group and others with different tracers supporting the use of ^{18}F-labelled tracers because of their better signal to noise ratio and also longer half-life allowing off-site use. It should be noted, however, that both the study of Dickens et al. [28] and ours uses models of strong and acute neuroinflammation. It would therefore be desirable to assess second generation TSPO tracers, such as [^{18}F]GE-180, [^{18}F]DPA-714, [^{18}F]PBR111, [^{18}F]FEDAA1106 and many others [15, 21], which have demonstrated better signal to noise ratio than [^{11}C]PK11195, using other types of model (e.g. multiple sclerosis, transgenic model of Alzheimer's disease) inducing lower levels of inflammation that are more challenging to detect.

Conclusion

The use of successive scans with ^{11}C-R-PK11195 and ^{18}F-GE-180 allowed us to truly compare the two tracers in the same animals, hence avoiding potential bias due to interindividual variability frequently observed in models such as the stroke model in rats. We were able to demonstrate that ^{18}F-GE-180 is a strong candidate for TSPO imaging with an improved signal to noise ratio and lower nonspecific signal when compared to ^{11}C-R-PK11195.

Acknowledgments This work was supported by GE Healthcare Ltd, the Wolfson Molecular Imaging Centre, Manchester, and the European Union's Seventh Framework Programme (FP7/2007–2013) under grant agreement HEALTH-F2-2011-278850 (INMiND). The authors thank the personnel of the Wolfson Molecular Imaging Centre, especially Miss Gemma Chapman and Messrs Marc Radigois and Michael Green for facilitating this study. The Bioimaging Facility microscopes used in this study were purchased with grants from BBSRC, Wellcome Trust, and the University of Manchester Strategic Fund. The authors also thank Peter March, Jane Kott and Robert Fernandez for running the Bioimaging Facility.

Disclosure This study was supported by GE Healthcare Ltd. GE Healthcare Ltd was involved in the design of the study and performed the metabolite analyses. GE Healthcare Ltd was not involved in other experiments.

References

1. Denes A, Thornton P, Rothwell NJ, Allan SM. Inflammation and brain injury: acute cerebral ischaemia, peripheral and central inflammation. Brain Behav Immun. 2010;24:708–23.
2. McColl BW, Allan SM, Rothwell NJ. Systemic inflammation and stroke: aetiology, pathology and targets for therapy. Biochem Soc Trans. 2007;35:1163–5.
3. Heneka MT, O'Banion MK, Terwel D, Kummer MP. Neuroinflammatory processes in Alzheimer's disease. J Neural Transm. 2010;117:919–47.
4. Johnston H, Boutin H, Allan SM. Assessing the contribution of inflammation in models of Alzheimer's disease. Biochem Soc Trans. 2011;39:886–90.
5. Lee YJ, Han SB, Nam SY, Oh KW, Hong JT. Inflammation and Alzheimer's disease. Arch Pharm Res. 2010;33:1539–56.
6. Holmes C, Cunningham C, Zotova E, Woolford J, Dean C, Kerr S, et al. Systemic inflammation and disease progression in Alzheimer disease. Neurology. 2009;73:768–74.
7. Akiyama H, Barger S, Barnum S, Bradt B, Bauer J, Cole GM, et al. Inflammation and Alzheimer's disease. Neurobiol Aging. 2000;21:383–421.
8. Lee JK, Tran T, Tansey MG. Neuroinflammation in Parkinson's disease. J Neuroimmune Pharmacol. 2009;4:419–29
9. Gerhard A, Pavese N, Hotton G, Turkheimer F, Es M, Hammers A, et al. In vivo imaging of microglial activation with [11C](R)-PK11195 PET in idiopathic Parkinson's disease. Neurobiol Dis. 2006;21:404–12.
10. Long-Smith CM, Sullivan AM, Nolan YM. The influence of microglia on the pathogenesis of Parkinson's disease. Prog Neurobiol. 2009;89:277–87.
11. Tansey MG, McCoy MK, Frank-Cannon TC. Neuroinflammatory mechanisms in Parkinson's disease: potential environmental triggers, pathways, and targets for early therapeutic intervention. Exp Neurol. 2007;208:1–25.
12. Ringheim GE, Conant K. Neurodegenerative disease and the neuroimmune axis (Alzheimer's and Parkinson's disease, and viral infections). J Neuroimmunol. 2004;147(1–2):43–9.
13. Banati RB, Newcombe J, Gunn RN, Cagnin A, Turkheimer F, Heppner F, et al. The peripheral benzodiazepine binding site in the brain in multiple sclerosis: quantitative in vivo imaging of microglia as a measure of disease activity. Brain. 2000;123(11):2321–37.
14. Oh U, Fujita M, Ikonomidou VN, Evangelou IE, Matsuura E, Harberts E, et al. Translocator protein PET imaging for glial activation in multiple sclerosis. J Neuroimmune Pharmacol. 2011;6:354–61.
15. Chauveau F, Boutin H, Van Camp N, Dollé F, Tavitian B. Nuclear imaging of neuroinflammation: a comprehensive review of [11C]PK11195 challengers. Eur J Nucl Med Mol Imaging. 2008;35:2304–19.
16. Venneti S, Lopresti BJ, Wiley CA. The peripheral benzodiazepine receptor (Translocator protein 18 kDa) in microglia: from pathology to imaging. Prog Neurobiol. 2006;80:308–22.
17. Pappata S, Cornu P, Samson Y, Prenant C, Benavides J, Scatton B, et al. PET study of carbon-11-PK 11195 binding to peripheral type benzodiazepine sites in glioblastoma: a case report. J Nucl Med. 1991;32:1608–10.
18. Turkheimer FE, Edison P, Pavese N, Roncaroli F, Anderson AN, Hammers A, et al. Reference and target region modeling of [11C]-(R)-PK11195 brain studies. J Nucl Med. 2007;48:158–67.
19. Folkersma H, Boellaard R, Vandertop WP, Kloet RW, Lubberink M, Lammertsma AA, et al. Reference tissue models and blood–brain barrier disruption: lessons from (R)-[11C]PK11195 in traumatic brain injury. J Nucl Med. 2009;50:1975–9.
20. Kropholler MA, Boellaard R, van Berckel BN, Schuitemaker A, Kloet RW, Lubberink MJ, et al. Evaluation of reference regions for (R)-[(11)C]PK11195 studies in Alzheimer's disease and mild cognitive impairment. J Cereb Blood Flow Metab. 2007;27:1965–74.
21. Dolle F, Luus C, Reynolds A, Kassiou M. Radiolabelled molecules for imaging the translocator protein (18 kDa) using positron emission tomography. Curr Med Chem. 2009;16:2899–923.
22. Tang D, McKinley ET, Hight MR, Uddin MI, Harp JM, Fu A, et al. Synthesis and structure-activity relationships of 5,6,7-substituted pyrazolopyrimidines: discovery of a novel TSPO PET ligand for cancer imaging. J Med Chem. 2013;56:3429–33.
23. Boutin H, Prenant C, Maroy R, Galea J, Greenhalgh AD, Smigova A, et al. [18F]DPA-714: direct comparison with [11C]PK11195 in a model of cerebral ischemia in rats. PLoS ONE. 2013;8:e56441.
24. Doorduin J, Klein HC, Dierckx RA, James M, Kassiou M, de Vries EF. [11C]-DPA-713 and [18F]-DPA-714 as new PET tracers for TSPO: a comparison with [11C]-(R)-PK11195 in a rat model of herpes encephalitis. Mol Imaging Biol. 2009;11:386–98.
25. Takano A, Piehl F, Hillert J, Varrone A, Nag S, Gulyas B, et al. In vivo TSPO imaging in patients with multiple sclerosis: a brain PET study with [18F]FEDAA1106. EJNMMI Res. 2013;3:30–3.
26. Takano A, Arakawa R, Ito H, Tateno A, Takahashi H, Matsumoto R, et al. Peripheral benzodiazepine receptors in patients with chronic schizophrenia: a PET study with [11C]DAA1106. Int J Neuropsychopharmacol. 2010;13:943–50.
27. Wadsworth H, Jones PA, Chau WF, Durrant C, Fouladi N, Passmore J, et al. [18F]GE-180: a novel fluorine-18 labelled PET tracer for imaging translocator protein 18 kDa (TSPO). Bioorg Med Chem Lett. 2012;22:1308–13.
28. Dickens AM, Vainio S, Marjamaki P, Johansson J, Lehtiniemi P, Rokka J, et al. Detection of microglial activation in an acute model of neuroinflammation using PET and radiotracers 11C-(R)-PK11195 and 18F-GE-180. J Nucl Med. 2014;55:466–72.

29. Calamante F, Lythgoe MF, Pell GS, Thomas DL, King MD, Busza AL, et al. Early changes in water diffusion, perfusion, T1, and T2 during focal cerebral ischemia in the rat studied at 8.5 T. Magn Reson Med. 1999;41:479–85.
30. Wegener S, Weber R, Ramos-Cabrer P, Uhlenkueken U, Sprenger C, Wiedermann D, et al. Temporal profile of T2-weighted MRI distinguishes between pannecrosis and selective neuronal death after transient focal cerebral ischemia in the rat. J Cereb Blood Flow Metab. 2006;26:38–47.
31. Camsonne R, Crouzel C, Comar D, Maziere M, Prenant C, Sastre J, et al. Synthesis of N-(11C) methyl, N-(methyl-1 propyl), (chloro-2 phenyl)-1 isoquinoleine carboxamide-3 (PK 11195): a new ligand for peripheral benzodiazepine receptors. J Labelled Comp Radiopharm. 1984;21:985–91.
32. Cremer JE, Hume SP, Cullen BM, Myers R, Manjil LG, Turton DR, et al. The distribution of radioactivity in brains of rats given [N-methyl-11C]PK 11195 in vivo after induction of a cortical ischaemic lesion. Int J Rad Appl Instrum B. 1992;19:159–66.
33. Maroy R, Boisgard R, Comtat C, Frouin V, Cathier P, Duchesnay E, et al. Segmentation of rodent whole-body dynamic PET images: an unsupervised method based on voxel dynamics. IEEE Trans Med Imaging. 2008;27:342–54.
34. Maroy R, Boisgard R, Comtat C, Jego B, Fontyn Y, Jan S, et al. Quantitative organ time activity curve extraction from rodent PET images without anatomical prior. Med Phys. 2010;37:1507–17.
35. Cawthorne C, Prenant C, Smigova A, Julyan P, Maroy R, Herholz K, et al. Biodistribution, pharmacokinetics and metabolism of interleukin-1 receptor antagonist (IL-1RA) using [18F]-IL1RA and PET imaging in rats. Br J Pharmacol. 2011;162:659–72.
36. Gerhard A, Schwarz J, Myers R, Wise R, Banati RB. Evolution of microglial activation in patients after ischemic stroke: a [11C](R)-PK11195 PET study. Neuroimage. 2005;24:591–5.
37. Thiel A, Radlinska BA, Paquette C, Sidel M, Soucy JP, Schirrmacher R, et al. The temporal dynamics of poststroke neuroinflammation: a longitudinal diffusion tensor imaging-guided PET study with 11C-PK11195 in acute subcortical stroke. J Nucl Med. 2010;51:1404–12.
38. Boutin H, Chauveau F, Thominiaux C, Gregoire MC, James ML, Trebossen R, et al. 11C-DPA-713: a novel peripheral benzodiazepine receptor PET ligand for in vivo imaging of neuroinflammation. J Nucl Med. 2007;48:573–81.
39. Chauveau F, Van Camp N, Dolle F, Kuhnast B, Hinnen F, Damont A, et al. Comparative evaluation of the translocator protein radioligands 11C-DPA-713, 18F-DPA-714, and 11C-PK11195 in a rat model of acute neuroinflammation. J Nucl Med. 2009;50:468–76.
40. Hughes JL, Jones PS, Beech JS, Wang D, Menon DK, Aigbirhio FI, et al. A microPET study of the regional distribution of [11C]-PK11195 binding following temporary focal cerebral ischemia in the rat. Correlation with post mortem mapping of microglia activation. Neuroimage. 2012;59:2007–16.